

The Lasers for Science Facility in the Research Complex at Harwell

Contact dave.clarke@stfc.ac.uk

David T Clarke

Central Laser Facility
Research Complex at Harwell

Marisa Martin-Fernandez

Central Laser Facility
Research Complex at Harwell

Mike Towrie

Central Laser Facility
Research Complex at Harwell

[The Lasers for Science Facility Team](#)

Central Laser Facility
Research Complex at Harwell

Introduction

The Research Complex at Harwell (RCaH), opened in July 2010, is a multidisciplinary laboratory that provides facilities to undertake new and cutting edge scientific research in both the life and physical sciences, and at the interface between them. RCaH operates as a partnership between STFC, MRC, BBSRC, EPSRC, NERC, and Diamond Light Source. STFC's major contribution to RCaH was the move of the LSF to the complex, begun at the end of 2009. The LSF completed its move to RCaH at the beginning of 2011, and is now operating a full user programme, including a growing number of new multidisciplinary and cross-facility projects working in collaboration with other RCaH residents.

Facilities

The main LSF facilities in RCaH are the ULTRA spectroscopy cluster and the OCTOPUS imaging cluster. These are described in detail in other articles. Briefly, each facility has a central laser "hub" which supplies laser light to a range of stations designed for advanced imaging and spectroscopy experiments. Techniques available include linear and non-linear Raman and IR spectroscopy, time-resolved resonance Raman spectroscopy, and transient 2D-IR spectroscopy (ULTRA), and single molecule microscopy, multiphoton/single photon confocal imaging, and fluorescence lifetime imaging (OCTOPUS). The LSF's facilities also include laser tweezers, a number of R & D labs, and support facilities for biology, chemistry, and spectroscopy. The EPSRC-funded laser loan pool, operated by the LSF, also operates out of RCaH. The layout of the LSF in RCaH is shown in Fig. 1 below.

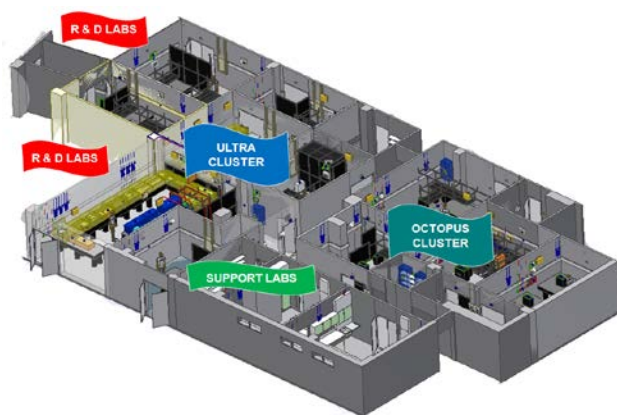


Fig. 1. The LSF within RCaH.

In addition to the LSF facilities, RCaH also houses a number of shared facilities including biochemistry, cell culture, and chemistry laboratories. Shared equipment available for use

includes a JEOL JEM-2100 transmission electron microscope with cryo specimen holder, JSM-6610LV scanning electron microscope, Bruker Avance III 400 400 MHz NMR spectrometer, and Agilent Supernova X-Ray diffractometer. A full list of shared equipment can be found on the RCaH website, <http://www.rc-harwell.ac.uk/>. This equipment is available for use by LSF users with prior arrangement.

RCaH is also home to the Oxford Protein Production Facility UK (<http://www.oppf.ox.ac.uk/>), which provides a protein production service for the research community, and CCP4 (<http://www.ccp4.ac.uk/>), providing data analysis software for macromolecular crystallography and other biophysical techniques. The Complex is also home to a growing number of life and physical sciences research groups, supported by the sponsoring Research Councils. The LSF is engaged in collaborative programmes with a number of these groups, some of which are detailed below.

Selected Multidisciplinary and Cross-Facility Programmes

Supra-molecular rules in signalling networks: A single molecule comparative study in cells and tissues. BBSRC; LSF/King's College London. This programme is jointly headed by Marisa Martin-Fernandez from the LSF and Prof. Peter Parker from KCL, and aims to develop new single molecule imaging techniques and apply them to the study of the networks that control cell survival and growth. The complexity of these networks means that it has been necessary to develop microscopes that are able to image and track a number of different molecular species simultaneously. A three colour microscope is now operational (Fig. 2), and a five colour microscope is being commissioned.

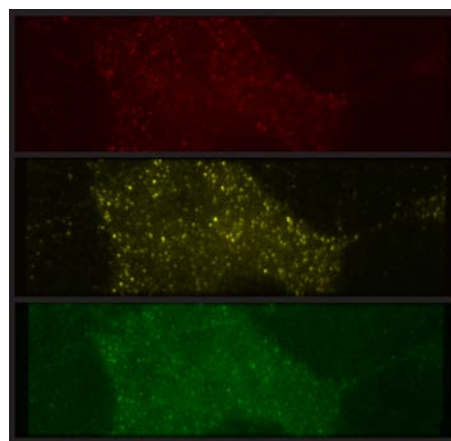


Fig. 2. . Simultaneous 3-colour single molecule TIRF imaging of HeLa cells labelled with EGF-Atto 647N (top); EGF-Alexa 546 (centre); and EGF-Atto 488 (bottom).

Data obtained from OCTOPUS microscopes are being analysed using new techniques being developed in collaboration with the astronomy community. These methods will allow us to identify and track single molecules in the noisy, high background environment of living cells. The combination of advanced laser microscopy, specialized analysis techniques, high-resolution structure from x-rays, and molecular dynamics simulation, allows us to build up a detailed picture of how proteins perform their functions in the cell. The effectiveness of this approach is shown in a recent publication in which the existence of a previously unknown conformation of the epidermal growth factor receptor was demonstrated¹. Ultimately, the goal is to apply these methods to the analysis of biopsies from tumours, enabling the best therapies to be selected for individual patients.

Dynamic structural science. EPSRC; consortium of 9 research organizations led by Bath University. This grant is one of four recently awarded by EPSRC for five-year multidisciplinary research projects in RCaH. It is led by Prof. Paul Raithby from Bath, with co-investigators from Nottingham, Leeds, Manchester, Durham, Southampton and Glasgow, as well as Mike Towrie from the LSF. The aim of the proposal is to develop ways to look at how molecules work in a range of materials where some structural change is vital in making the materials function. This can include protein molecules in the body, materials whose optical properties change in sensors and those whose ability to conduct electricity can change when used in computer chips. This is a hard task, as the processes where molecules change can be very fast, and we need to use advanced experimental methods to achieve this aim. In order to achieve this, the plan is to use a combination of techniques that are available on the campus, including ultrafast time-resolved spectroscopy on the LSF's ULTRA facility, time-resolved x-ray diffraction and EXAFS on Diamond, and time-resolved neutron scattering on ISIS. The team will use their combined expertise to develop all these approaches to a new level of sophistication and apply them to key problems of chemical and biological importance, such as watching an optical sensor material function on a μs timescale or follow the functional conformational changes of macromolecules over the ps- μs time domains.

Structural evolution across multiple time and length scales. EPSRC; led by Manchester with contributions from Imperial, STFC, and OU. A second EPSRC multidisciplinary research at RCaH grant, led by Prof. Philip Withers from Manchester, with a number of co-investigators including Dave Clarke from the LSF. The project aims to take advantage of the unprecedented opportunity to obtain information about material structure and behaviour using the suite of synchrotron and lab X-ray, neutron, laser, electron, and NMR imaging available at Harwell. This infrastructure provides an opportunity to undertake science changing experiments. The goal is to bring together the insights from different instruments to follow structural evolution under realistic environments and timescales to go beyond static monochrome 3D images by radically increasing the dimensionality of information available. We will:

Derive 4D imaging algorithms to access shorter timescales for time series (structure+time)

Enable colour/chemical imaging (structure+time, chemistry)

Establish correlative X-ray imaging (structure+chemistry, functionality, etc)

Establish In situ Environments and Tissue Regeneration Labs. in the Research Complex

These will radically increase the level of information that can be obtained from a sample, or process, delivering both academic and industrial benefits over a very wide variety of fields. In particular we will focus our experiments relating to Energy and Biomaterials. Key challenges we aim to meet:

- Following tissue regeneration in soft and hard biomaterials having fibrous and porous architectures using multiple imaging modalities.
- Studying solid oxide fuel cells during operation at the sub-micron scale for the first time.
- Studying fluid flow, including supercritical CO₂, through porous rocks for oil recovery and carbon capture.
- Obtaining first insights into oxidation of turbine materials in 3D under their extreme operating conditions.

The LSF will participate in this programme through the use of multiple imaging modalities available in the OCTOPUS cluster.

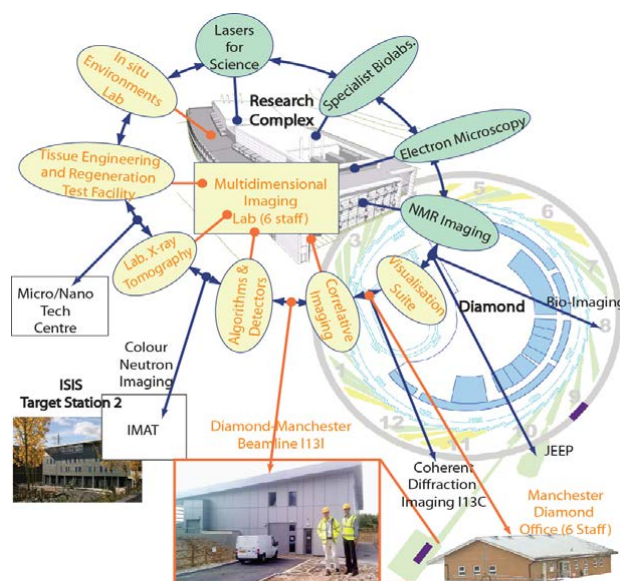


Fig. 3. Imaging facilities available on the campus that will be used in the Manchester programme.

The EPSRC awarded two other RCaH multidisciplinary research grants. These also have significant requirements in the imaging and spectroscopy areas and collaborations are currently being formed with members of the LSF team.

Other LSF programmes. The programmes described above are just a few examples from the current research portfolio of the LSF. Other research includes the development of new methods for studying ultrafast protein dynamics, looking at the dynamics of energy storage systems, investigating new methods for cancer therapy and diagnosis, and looking at the chemistry of clouds. An overview of the LSF's activities can be obtained from the [current user schedule](#).

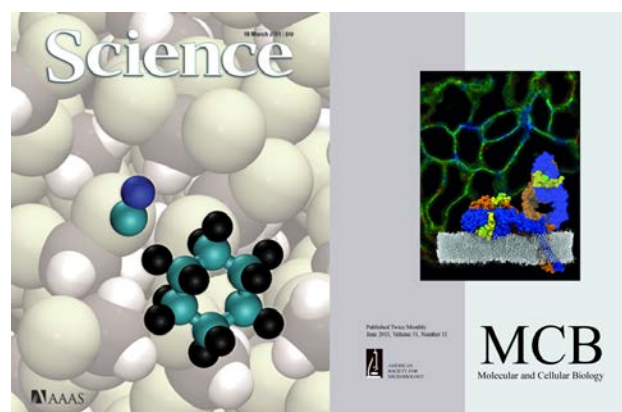


Fig. 4. Recent front covers from the LSF.

Of particular note is the growing number of experiments requiring access to other facilities in addition to the LSF, with

17 ongoing and planned collaborative programmes at the time of writing involving Diamond, ISIS, and other campus partners. Some selected recent publications from the LSF can be found below²⁻⁷, the quality of the research being demonstrated by two front cover articles, one of them in *Science*. The EPSRC-funded laser loan pool also continues to go from strength to strength, lending 8 systems including two new ones, resulting in many publications including a recent one in *Nature*⁸.

Conclusions

The last few years have been busy ones for the LSF, with a move to RCaH, an increased focus on programmatic and multidisciplinary research, and the commissioning of two world-class facilities, ULTRA and OCTOPUS. The facility supports an active and growing science programme in many areas, (supported by 50 active grants from UK Research Councils with a total value of £42M) and is increasingly in demand from users of other campus facilities. We look forward to seeing more exciting science from the facility as the campus interactions strengthen and new groups take up residence in the Research Complex.

Acknowledgements

The research programme described in this article would not have been possible without the entire LSF team. Ideally they would all have been named authors on this article but this is not possible because of space constraints. Details of the team can be found [here](#). We would also like to thank the CLF engineering division for all their work in ensuring a successful move of some very complex facilities to a new building. Finally, we would like to thank the Director of RCaH, Simon Philips, and his team for their help and support since we have been RCaH residents.

References

1. C. J. Tynan, S. K. Roberts, D. J. Rolfe, D. T. Clarke, H. H. Loeffler, J. Kastner, M. D. Winn, P. J. Parker and M. L. Martin-Fernandez, *Mol Cell Biol* **31**, 2241-2252 (2011).
2. S. J. Greaves, R. A. Rose, T. A. Oliver, D. R. Glowacki, M. N. Ashfold, J. N. Harvey, I. P. Clark, G. M. Greetham, A. W. Parker, M. Towrie and A. J. Orr-Ewing, *Science* **331** (6023), 1423-1426 (2011).
3. P. M. Keane, M. Wojdyla, G. W. Doorley, G. W. Watson, I. P. Clark, G. M. Greetham, A. W. Parker, M. Towrie, J. M. Kelly and S. J. Quinn, *J Am Chem Soc* **133** (12), 4212-4215 (2011).
4. N. T. Hunt, G. M. Greetham, M. Towrie, A. W. Parker and N. P. Tucker, *Biochem J* **433** (3), 459-468 (2011).
5. A. Jeshtadi, P. Burgos, C. D. Stubbs, A. W. Parker, L. A. King, M. A. Skinner and S. W. Botchway, *J Virol* **84** (24), 12886-12894 (2010).
6. S. W. Botchway, A. M. Lewis and C. D. Stubbs, *Eur Biophys J* **40** (2), 131-141 (2011).
7. T. M. Ismail, S. Zhang, D. G. Fernig, S. Gross, M. L. Martin-Fernandez, V. See, K. Tozawa, C. J. Tynan, G. Z. Wang, M. C. Wilkinson, P. S. Rudland and R. Barraclough, *Journal of Biological Chemistry* **285** (2), 914-922 (2010).
8. E. J. Cocinero, P. Carcabal, T. D. Vaden, J. P. Simons and B. G. Davis, *Nature* **469** (7328), 76-79 (2011).

Contact Benjamin.Coles@stfc.ac.uk

Benjamin Coles
Central Laser Facility
Research Complex & Harwell

Mike Towrie
Central Laser Facility
Research Complex & Harwell

Tony Parker
Central Laser Facility
Research Complex & Harwell

Gregory M. Greetham
Central Laser Facility
Research Complex & Harwell

Alexandra Lauer
Chemistry Dept.
Oxford University

Phillip Kukura
Chemistry Dept.
Oxford University

Ian P. Clark
Central Laser Facility
Research Complex & Harwell

Pierre Burgos
Central Laser Facility
Research Complex & Harwell

6 μm Thick Open Flow “Wire Guided” Liquid Jet

Introduction

In time resolved pump-probe spectroscopy the high flux and power of the lasers can lead to unwanted background signals from non-linear optical processes induced in the window and/or photo-degradation of sample at the window fluid interface. An open flowing jet of solution can get round these problems.

Figure 1a

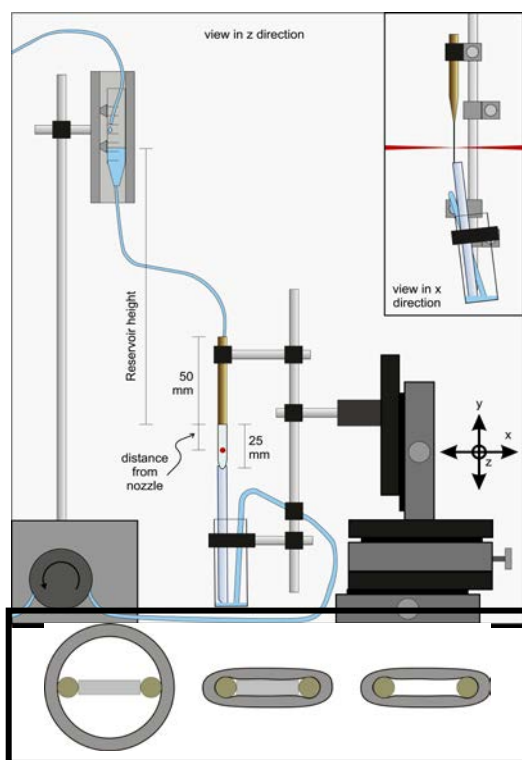


Figure 1b

and solutions.

Figure 1a shows the experimental configuration. A nozzle based on a 5 cm length of stainless steel pipe (2.2 mm I.D. and 0.5 mm wall thickness) is squeezed at one end over a 6-7 cm length loop of 0.125 mm diameter tantalum wire, (see figure 1b). A metal insert and custom tool is used to prevent crushing of the pipe. The insert is removed once the wire is in place. The wire is fashioned into a U-shape with straight parallel sides down which the solution runs. The solution flows by gravity feed from a reservoir via a ~1 mm I.D. PTFE pipe (20-50 cm) down through the nozzle and along the wires (guided by surface tension). The end of the wire loop is set to touch the edge of a glass pipe (see insert in figure 1b) that stops build up of fluid at the end of the loop and collects the solution into a lower reservoir. A Masterflex all PTFE peristaltic pump then pumps the

can get round these problems. However, it is challenging to create a stable thin jet using low viscosity volatile solvents. One method is to use a thin wire to guide the flow of the fluid and this approach has been applied in time resolved experiments [1].

Experimental setup

Here we report the design and characterisation of a flow cell that has been used in experiments on the ULTRA laser system with acetonitrile and cyclohexane solutions and should be suitable for a wide range of low to medium viscosity solvents

solution back to the upper reservoir to complete the cycle. The rate

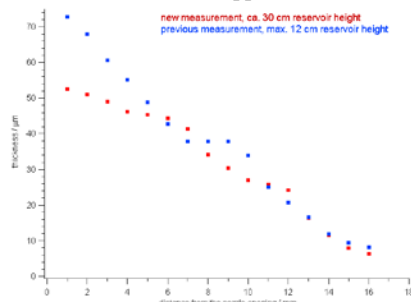


Figure 2

of flow is controlled by adjusting the height of the upper reservoir relative to the nozzle. Jet thickness and stability were measured using a dye solution of known absorbance and a focused HeNe laser passing through the sample (see insert figure 1a). Figure 2 gives the measured thickness of the jet for 15 and 30 cm upper reservoir heights. At 1 mm below the nozzle output the thickness is 74 and 53 μm respectively falling to around 6 μm s at 16 mm below the nozzle output.

Performance

Measurements on the stability of the jet at 6 μm thickness were carried out by recording the intensity of the HeNe (at about 40% absorption in the dye solution). Fluctuation at the +/- 15% level in the sub 100 Hz frequency range was measured; this dropped to less than +/-0.4% around 5 kHz the frequency at which ULTRA detects signals. At this level these fluctuations will not contribute significantly to noise in the time resolved spectroscopy measurements.

As an example of the application of the jet figure 3 shows the femtosecond stimulated Raman spectra of cyclohexane in the C-H stretching region of the spectrum taken at the top (~70 μm thick) and bottom (~6 μm thick) of the jet. Good spectra were taken with pump energies of 20 μJ . This pump energy could not have been used in a cell with windows as it is well above the threshold for non-linear plasma breakdown in window materials.

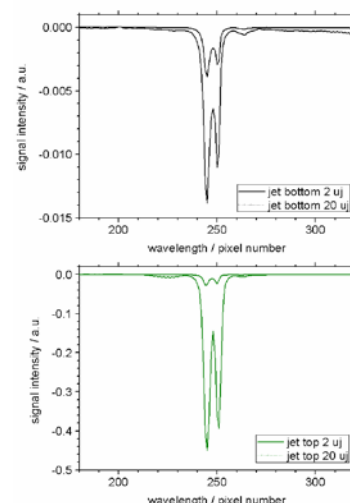


Figure 3

Conclusion

It has yet to be determined whether this jet can be used for time resolved IR spectroscopy as interference of Fresnel reflections of the surfaces may become more of a problem in the IR. However, the jet is suitable for time resolved Raman spectroscopy, both fs-stimulated Raman and time resolved Resonance Raman (TR³), and for transient absorption measurements in the UV – visible.

Closed flow-cell system using low volume samples

Introduction

The use of a peristaltic pump is a common method of circulating samples through a flow cell. However, this imposes several limitations; namely restricting the minimum sample volume to that of the tubes, and the requirement to use a flexible tubing type, which may not be amenable to the sample solvent or temperature (e.g. for extremely low temperature measurements that can harden and damage the tubing used in the pump).

A conference paper^[2] proposes a method of overcoming these limitations by employing pressurized gas in place of the traditional pump and using a level monitoring system to cycle the sample through the flow cell.

Experimental setup

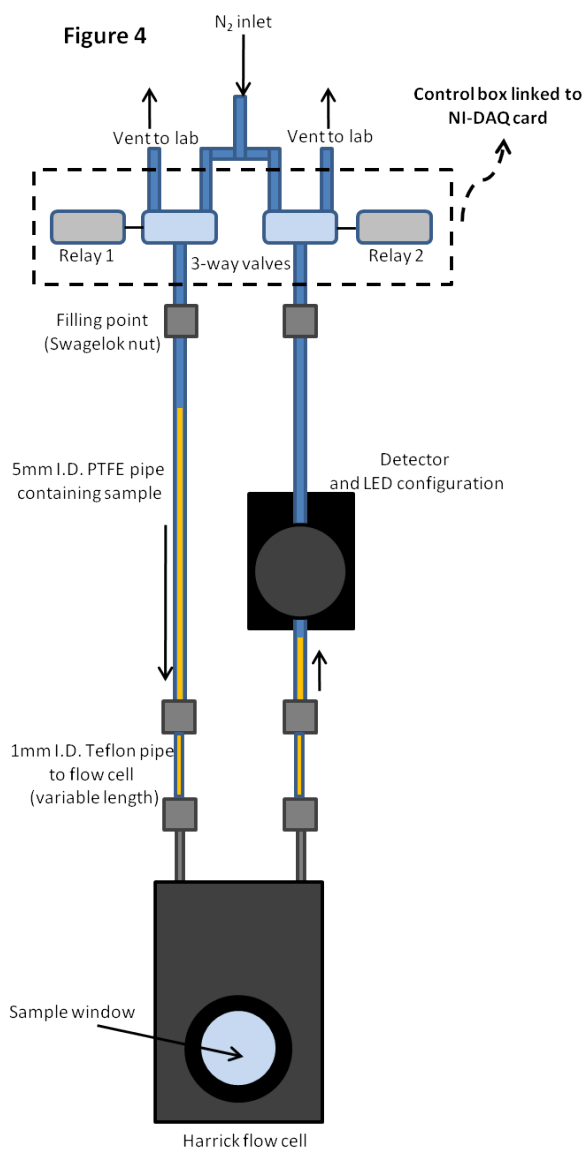
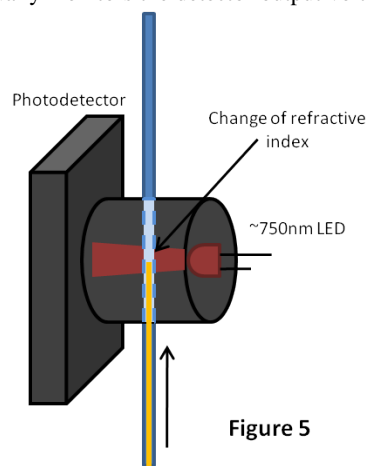


Figure 4 illustrates the experimental configuration. A variable pressure nitrogen source (0 - 5 bar) is split into two 3-way solenoid valves. The valves are arranged with one venting to room whilst the other pressurises the flow system, driving the sample through the flow cell. Switching between the two valves allows the direction of flow to be changed.

The flow monitoring system comprises of a visible wavelength photodetector attached to the PTFE tube directly opposite the fill nut. Figure 5 shows an enclosed LED, emitting light onto the detector. The LED emits light at ~750nm which is at the peak efficiency of the detector, and also reduces backward scattering from the sample. The voltage output of the detector is fed into a National Instruments Data Acquisition (NI-DAQ) card which is in turn controlled by LabVIEW. The NI-DAQ card also controls the relays driving the valves, and provides power to the LED.

LabVIEW software continually monitors the detector output voltage. The change in refractive index caused by the rising sample causes the output voltage of the detector to rise. Once this voltage rises above a predetermined trigger threshold, LabVIEW software controls simultaneously switching of the valve relays.



This event starts an adjustable timer, which measures the amount of time elapsed whilst the sample is being driven back towards the fill nut. Once the timer reaches its predetermined value, LabVIEW software controls switching of the relays back to their original position, restarting the cycle.

The nitrogen pressure, voltage and time thresholds can be adjusted to meet the desired flow speed and to ensure the entire volume is cycled through the flow cell on each repetition.

Effectiveness

This system has so far proved effective with water and common solvents with minimum bubble formation, though hysteresis could be introduced to the feedback mechanism with more viscous samples. Background light does affect the threshold trigger voltage and so the system only works if this is held constant, preferably enclosed. The flow system has a finite switching time in the order of tens of milliseconds, which would need to be factored into designing flow-cell experiments using this technique, with the potential to integrate the LabVIEW control software with acquisition software to avoid switching during acquisition periods.

The flow system provides solutions to many of the issues faced when using a traditional peristaltic pump. The PTFE tubes and stainless steel connectors make the system more resistant to degradation, and the system works under nitrogen, preventing sample oxidation. The high pressure rated PTFE tubes allow extremely fast cycle times, with a potential to achieve >1 Hz.

The whole length of sample tube can be submerged in a water/dry-ice bath, enabling temperature extremes to be sustained, for example temperatures of less than -50°C are possible. The tubes are also easy to clean and replace between experiments if necessary.

Future improvements

Once the capability of the flow system has been demonstrated, further improvements to the system can be made to increase the functionality and effectiveness.

The nitrogen inlet could be put through a bubbler to ensure that it has saturated vapour of the solvent in order to minimise sample evaporation.

A reservoir placed before each 3-way valve would prevent a vent overflow in the event of a feedback mechanism failure, which would avoid damaging the valves and having the sample leak inside the control box.

A near Infra-red LED and sensor could also be used in order to further reduce scattering, and an extra photo-sensor could also be employed to negate the need for a timed return cycle.

References

1. Tauber MJ, Mathies RA, Chen XY, et al., 'Flowing liquid sample jet for resonance Raman and ultrafast optical spectroscopy'. *Review of Scientific Instruments*, **74**, 11, pp4958-4960 (2003).
2. Alexoff DL, Hallaba K, Scler D, Ferrieri R, et al., 'A simple liquid detector for radiopharmaceutical processing systems', paper presented at 5. International workshop on targetry and target chemistry, Upton, NY (United States), 19-23 Sep 1993.

Signal Dependence on Depth in Transmission Raman Spectroscopy

Contact Pavel.Matousek@stfc.ac.uk

Pavel Matousek

Central Laser Facility
STFC Rutherford Appleton Laboratory, OX11 0QX

David Littlejohn, Alison Nordon

WestCHEM, Department of Pure and Applied Chemistry and
CPACT, University of Strathclyde, Glasgow G1 1XL

Neil Everall

Intertek-MSG
The Wilton Centre, Wilton, Redcar, TS10 4RF

Matthew Bloomfield

Cobalt Light Systems Ltd
The Electron Building, Fermi Avenue, Oxfordshire, OX11 0QR

Introduction

Transmission Raman spectroscopy (TRS) is currently being established as a valuable tool for analysing volumetrically the chemical content of intact pharmaceutical formulations.^{1,2,3} Key advantages over conventional backscattering Raman spectroscopy include the effective suppression of the sub-sampling effect.² Additional benefits include the ability to suppress Raman and fluorescence signals originating from surface layer of the sample compared with conventional Raman spectroscopy.^{3,4} Here, we investigate the dependence of the transmission Raman signal on the depth of its origin. This issue is of particular relevance to the quantification of highly heterogeneous formulations or multi-layer or multi-core tablets. Ideally, the contribution of individual (hypothetical) layers within a pharmaceutical tablet to the overall detected Raman signal should be uniform, i.e. the signal is depth insensitive. However in reality, some dependence of TRS signals on depth is present although by many orders of magnitude lower level in comparison with that of conventional backscattering Raman spectroscopy.² This remaining bias is often of little relevance unless highly heterogeneous formulations are present, such as with multi-core tablets or multi-layer tablets. The presence of this bias was also reported experimentally by Townshend *et al*⁵, Johansson *et al*⁶ and Everall *et al*⁷. The previous studies analysed basic situations involving bare, non-absorbing pharmaceutical tablets. Here we considerably broaden the scope of investigations including also the effect of a recently developed 'photon diode' signal enhancing element.

The photon diode is an optical element capable of boosting overall transmission Raman signals from pharmaceutical tablets typically by up to an order of magnitude and improving the signal-to-noise ratio (s/n) of the generated TRS spectra.⁸ The optical element acts as a special 'unidirectional mirror' located in close proximity to the sample over the laser illumination zone. The role of the element is to prevent the loss of diffusely scattered photons from the sample over a typically extended laser illumination zone, whilst permitting the laser beam to be transmitted into the sample through the optical element unimpeded. The concept relies on the generic angular properties of dielectric filters for which the spectral transmission profile shifts to shorter wavelengths for photons impacting them at angles further away from normal incidence. The enhanced coupling of laser radiation into the sample leads to a substantial boost of the overall Raman signal generated within the sample.

A full account of this work is given in Ref⁹.

Numerical Simulations

Monte Carlo simulations were used to study the TRS signal dependence on depth within a pharmaceutical tablet under various conditions. The model used was described in detail

earlier.⁸ It considers the sample to be a homogeneous turbid medium with one sample-to-air interface located at the top surface $z=0$, where z is a Cartesian coordinate normal to the interface plane. Other sample-to-air interfaces exist at the opposite side of the sample at the position $z=d$, where d is the sample thickness, and on its sides. The sample is chosen to have a round shape with a diameter of 12 mm mimicking a typical pharmaceutical tablet. A tablet thickness of 5 mm was used unless stated otherwise.

The model assumes that all the laser photons are first placed at a depth below the surface equal to the transport length l_t and symmetrically distributed around the origin of the coordinate system x,y . The beam diameter of the incident laser light was assumed to be 6 mm (unless stated otherwise) and the beam was of a uniform intensity across its cross section, i.e. it had a flat, 'top-hat' intensity profile with all the photons having equal probability of being injected into the sample at any point within its cross-section. The Raman light was collected at the sample surface in the transmission geometry from the opposite side of the sample, symmetrically around the projection axis of the collection/laser illumination area of 6 mm in diameter.

The sample was subdivided into 20 layers, each 250 μm thick, unless indicated otherwise. The origin of each generated Raman photon was recorded. Only the Raman photons emerging within the collection aperture were counted as detected and the analysis included the evaluation of the contribution of individual layers towards the overall Raman signal.

The numerical code was written in Mathematica 5.0 (Wolfram Research). 100,000 photons were propagated simultaneously, each across an overall distance of 1000 mm after which the calculations were stopped. The optical density accounting for the conversion of laser photons into Raman photons was set to 1 per 2 m. The step size used was $t = 0.2$ mm. The calculations were repeated 10 times summing all the detected Raman photons in the repeated runs.

Experimental

The experimental study was performed using a commercial transmission Raman instrument (TRS100, Cobalt Light Systems Ltd) operating at 830 nm with the power set to 800 mW at the sample. The acquisition time in all the measurements was 10 s (10 x 1s). The laser illumination spot diameter was 2 mm and the Raman signal was collected from a 6 mm diameter area on the surface of the sample in the transmission geometry.

The sample comprised eight stacked 0.5 mm thick discs resulting in an overall tablet thickness of 4 mm. Each disc was fabricated by compressing Avicel microcrystalline cellulose (MCC). A poly(ethylene terephthalate) (PET) foil of thickness 330 μm and diameter ~ 13 mm was inserted into different depths

within the segmented tablet. The foil contained ~ 18% of TiO₂ (anatase) filler, making it a highly turbid medium with a strong Raman signal that was easily monitored. An area under a TiO₂ band at ~140 cm⁻¹ was used to evaluate the strength of the Raman signal from the foil. The Raman signal was then normalised by dividing it with the overall matrix (MCC) signal intensity derived from an area under the neighbouring MCC Raman bands at 310-390 cm⁻¹.

The photon diode enhancer was placed at the bottom of the stack centred over the laser illumination zone. As a precaution its active dielectric layer was oriented towards the laser (i.e. away from the tablets) to minimise a risk of its potential mechanical damage by the tablet. This orientation somewhat reduced its effectiveness, although it still permitted a considerable enhancement to be induced. The beam enhancer in this configuration and with this sample yielded an overall Raman signal enhancement factor of 6.3.

Numerical Results – Bare Tablet

Figure 1 shows the contribution of individual layers within a tablet towards the overall collected Raman signal (see Fig 1). The appearance of noise-like features on the top of the overall profile is an artefact stemming from the photon shot-noise nature of the simulations. In general terms, the profile has a maximum close to the centre of the tablet and gradually decreases towards each face of tablet. The decrease is initially shallow but steepens out towards the air-to-sample interfaces. The bias towards the centre of tablet was stronger than predicted in our original simulations, but agrees very well with other Monte Carlo¹⁷ and experimental^{5,16,17} results. The presence of this phenomenon is ascribed to the loss of photons to the air at the interfaces, reducing the overall photon density in the proximity of the interfaces. In this context, signals in NIR absorption spectroscopy would be subject to similar processes and as such exhibit an analogous dependency.

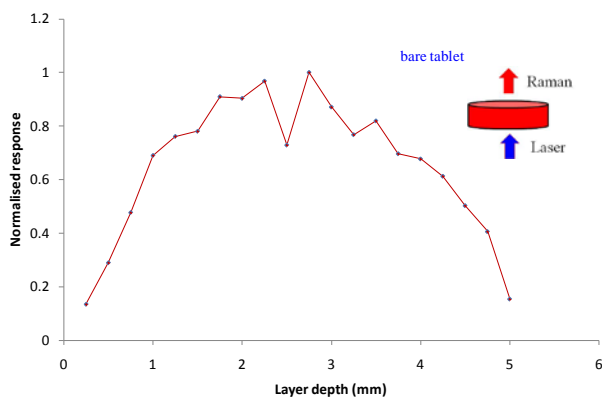


Figure 1: Numerical simulations of the dependence of Raman signal on the depth of its origin within a bare tablet.

Numerical Results – Tablet with Photon Diode

Figure 2 shows the depth dependence profiles with ($R > 0$) and without ($R = 0$) the photon diode. Several scenarios for different reflectivity levels of the optical element are analysed. Here, the enhancer reflectivity accounts for the combined effect of the reflectivity of the dielectric layer, as well as small loss of photons escaping from the sample through the filter within an angular cone at near normal incidence, direction resulting from the finite spectral bandwidth of the photon diode.⁸ It is evident that the increased reflectivity of the enhancer, apart from enhancing the overall Raman signal intensity, also lifts the depth profile up preferentially near the tablet surface where the enhancer is deployed (the depth is measured from the surface of the tablet illuminated by the laser).

An interesting situation arises with a reflectivity $R = \sim 0.8$ when the signal exhibits a semi-plateau dependence becoming

insensitive to the depth over the most of the tablet depth apart from a region near the Raman collection surface. Here, the signal depth profile is mostly unaffected by the presence of the enhancer. Further increase of the reflectivity to $R = 0.95$ then leads to the over representation of the front face of the tablet (the side illuminated by the laser). From this analysis it is evident that by controlling the reflectivity of the photon diode, one can also control the flatness of the depth dependence curve; the most favourable situation arising with a reflectivity of ~ 0.8 under the given conditions.

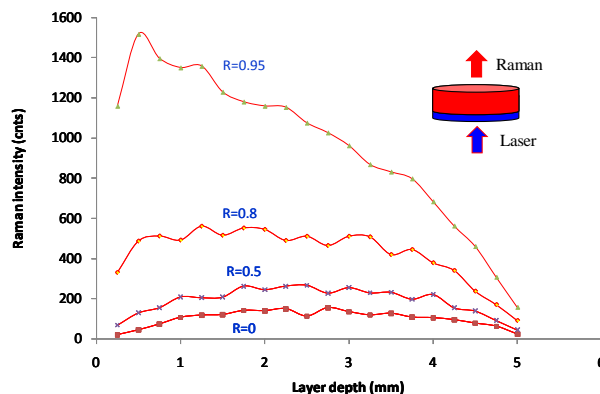


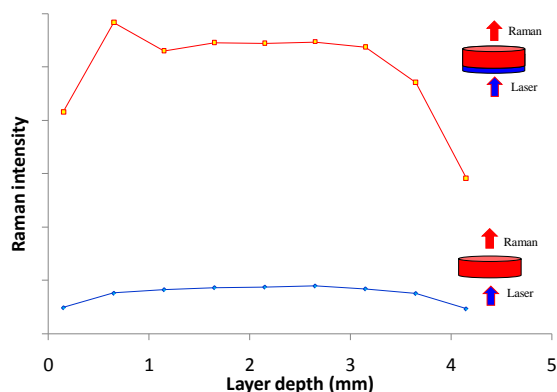
Figure 2: Numerical simulations of the dependence of Raman signal on the depth of its origin within a bare tablet and tablets with signal enhancing photon diode applied to the laser illumination side (a depth of 0 mm corresponds to the laser illumination side of tablet). The reflectivity (R) of the photon diode is indicated next to the curves.

Experimental Results

The dependence of the Raman signal on depth was also investigated experimentally for two key scenarios; with the signal enhancing photon diode and for a bare tablet. In these experiments a stack of eight 0.5 mm discs of microcrystalline cellulose (MCC) was used with a thin PET foil doped with TiO₂ inserted at different depths. For practical reasons the experimental demonstration was performed under somewhat different conditions from the previous simulations, with a thinner overall tablet thickness and using a different laser beam diameter from that of the Raman collection area. To permit the direct comparison between the experiment and theory the numerical simulations were repeated using the same parameters as those in the experiments. In these Monte Carlo simulations the laser beam illumination zone diameter was assumed to be 2 mm and the Raman collection diameter was 6 mm. The overall tablet thickness was 4 mm subdivided into 8 layers (each 0.5 mm thick) and tablet diameter 13 mm.

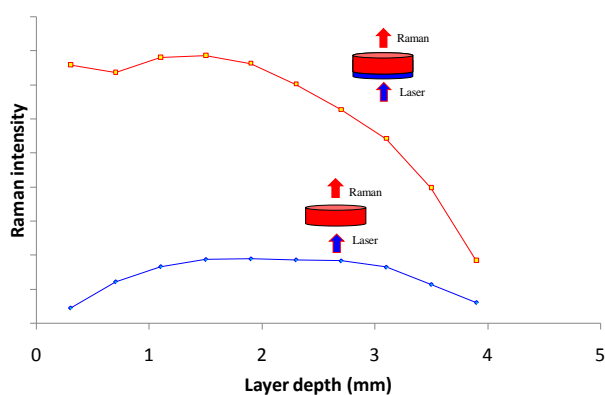
The results of the simulation are shown alongside the experimental results in Figure 3 showing the dependence of the PET foil TRS signal on its depth within the stacked tablet. In regard to the bare tablet, it is evident that the main features of the simulated profile were qualitatively reproduced experimentally: the bias towards the centre of the tablet, the symmetry of the curve, the presence of a flatter region in the central part of sample, and a steeper drop near the air-to-sample interfaces. In terms of notable differences, the experimental curve exhibits a somewhat shallower response compared with the theoretical one. The depth dependence is contained with 50% of the maximum for the experimental curve whereas the theoretical curve shows more prominent drop off towards the edges of tablet. The reason for this discrepancy is not fully clear but is likely to be due to a simplified nature of the model and assumptions made that do not faithfully reproduce all the features of experiment. In practical terms the shallower curve that is present in real situations is naturally beneficial to quantitative volumetric sampling, as it provides larger insensitivity to the depth and consequently facilitates more uniform averaging of signals across the tablet volume.

Experiment



a)

Monte Carlo simulations



b)

Figure 3: Comparison of (a) experimental and (b) numerical dependences of Raman signal on the depth of its origin within a bare tablet and a tablet with an enhancing element applied to the laser incident side.

Figure 3 also illustrated the effect of the photon diode element on the depth dependence profile. The numerical simulations assumed a photon diode reflectivity of $R=0.9$. The results of both the experiment and numerical simulations indicate the presence of enhancement that is larger on the laser incident side of the sample where the optical element is present. Somewhat smaller overall enhancement was yielded by the model than that observed experimentally implying again an imperfect match between the model and the experiment. Both the numerical and experimental results also provide evidence of the formation of a flatter response between the middle point and the photon diode part of the sample. As in the case of a bare tablet above, a notably flatter response was present in the experimental results compared with the numerical simulations.

Conclusions

The numerical simulations confirm the presence of a moderate bias of the transmission Raman signal towards the centre of the tablet. The deployment of a signal enhancing photon diode is shown to have a dual benefit: it enhances the Raman signal and its signal to noise ratio overall as well as providing an ability to control the flatness of the depth dependence curve. With appropriately optimised reflectivity, one can produce a considerably flatter depth response curve than that present for a bare tablet. This property can be used to provide more uniform signal averaging across the tablet volume contributing to a higher accuracy of volumetric quantification. This is particularly beneficial when highly heterogeneous samples are used. These findings were also substantiated experimentally on

a segmented tablet by inserting a PET film at different depths and monitoring its signal strength relative to the overall transmission Raman signal from the tablet matrix as a function of its depth.

It should be noted that in most studies the observed signal dependence on depth, which is of a moderate magnitude, will not have a major practical bearing on the quantification of pharmaceutical formulations apart from special cases such as with two-layer tablets or extremely heterogeneous formulations (e.g. tablets with lumps of active ingredients or excipients). In such cases the deployment of a signal enhancing photon diode may be required to control the uniformity of the signal depth response curve.

Acknowledgements

The Royal Society is thanked for the award of a University Research Fellowship to AN.

References

1. P. Matousek and M.D. Morris, *Emerging Raman Applications and Techniques in Biomedical and Pharmaceutical Fields*, Springer, Heidelberg, 2010.
2. P. Matousek and A.W. Parker, *Appl. Spectrosc.* 60, 1353 (2006).
3. P. Matousek and A.W. Parker, *J. Raman Spectrosc.* 38, 563 (2007).
4. K. Buckley and P. Matousek, Recent advances in the application of transmission Raman spectroscopy to pharmaceutical analysis, *J. Pharm. Biomed. Anal.*, in print (2011), DOI:10.1016/j.jpba.2010.10.029.
5. N. Townshend, D. Littlejohn, A. Nordon, M. Myrick, J. Andrews and P. Dallin, *PhAT Raman analysis of pharmaceutical tablets*, unpublished study, (2009).
6. J. Johansson, O. Svensson, S. Folestad, A. Sparen and M. Claybourn, *Transmission Raman Spectroscopy for Robust Tablet Assessment*, FACSS Conference Proceedings, Abstract 300 (Louisville, Kentucky, 2009), p. 131.
7. N. Everall, I. Priestnall, P. Dallin, J. Andrews, I. Lewis, K. Davis, H. Owen and M.W. George, *Appl. Spectrosc.* 64, 476 (2010).
8. P. Matousek, *Appl. Spectrosc.* 61, 845 (2007).
9. P. Matousek, N. Everall, D. Littlejohn, A. Nordon, M. Bloomfield, *Appl. Spectrosc.* (2011), in print.

Improvement of laser tweezer experiments using kHz-rate feedback control

Contact mark.pollard@stfc.ac.uk

M Pollard, I Brawn, S W Botchway, A Clark, E Freeman, R N J Halsall, A W Parker, M Towrie, R Turchetta & A D Ward
Science & Technology Facilities Council, Central Laser Facility, Rutherford Appleton Laboratory, Harwell Science and Innovation Campus, Oxfordshire OX11 0QX

Introduction

Laser tweezers provide precise control of microscopic particles with applications in several scientific disciplines particularly in the life sciences where processes that occur at the cellular level in liquid environments can be investigated. Extremely small forces ($< 10^{-12}$ N) can be detected by measuring the motion of the controlled particles, but this motion is disturbed by thermally-generated collisions with other particles (known as Brownian motion).

We report a feedback control system that reduced these unwanted perturbations in 6 particles by tracking their positions to nanometre accuracy and by adjusting the laser tweezers position accordingly to restore the particles to their desired positions. The system described here used high speed electronics (a field programmable gate array or FPGA) that was developed in collaboration with the STFC Technology department to perform tasks such as imaging, position measurement and laser control.

Position measurement and laser control

The laser tweezers apparatus (see Figure 1) included a microscope with an objective lens (x60 magnification, numerical aperture 1.2) that focused an infra-red, continuous-wave laser beam to control the microscopic particles. Up to six microscopic spheres were controlled by scanning the laser beam rapidly at > 10 kHz between positions using an acousto-optic deflector (AOD).

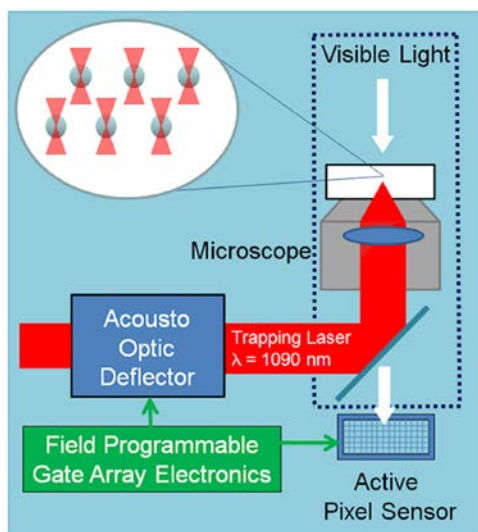


Figure 1. Diagram of laser tweezer and imaging apparatus

The positions of the microscopic spheres were measured using visible light (from the microscope lamp) and imaged on to an active pixel sensor [1], which generated images of the spheres at a rate of 14 k frames / second. The FPGA controlled the active pixel sensor, processed the sensor images to find the position of the spheres and adjusted the position of the tweezing laser beam via the AOD.

Control system

The control system used a feedback loop that was performed by the FPGA (shown in Figure 2) where changes in

sphere position (x_B) caused by unwanted Brownian motion were compensated by repositioning the laser beam (x_T) to exert a greater force to restore the spheres back to a set-point. The magnitude of the trap repositioning was controlled by a gain value (k). At each stage of the loop, the same operation was performed for all six spheres. The total time delay from image acquisition to trap reposition was $140 \mu\text{s}$, with the FPGA electronics providing the necessary speed and synchronisation of the loop. This speed enabled subsequent experiments that measured forces at sub-millisecond timescales.

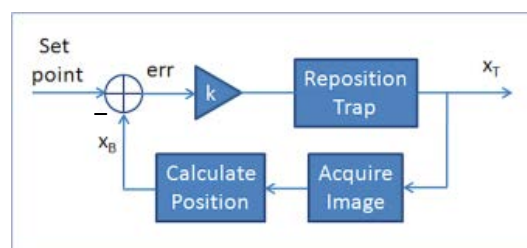


Figure 2 Diagram of the feedback loop within the control system.

Results

The feedback control system was applied to reduce the unwanted position variation in an optically-controlled microsphere (with $5 \mu\text{m}$ diameter) by 60 %, as shown in Figure 3.

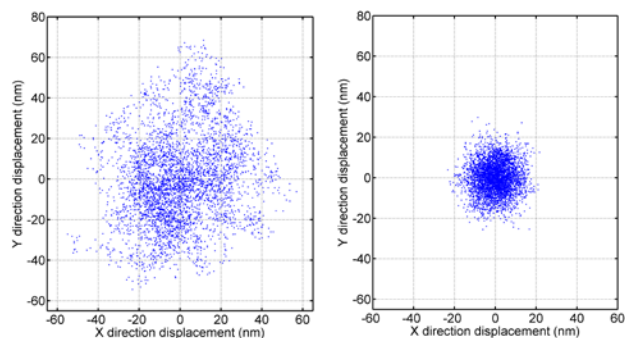


Figure 3. Scatter plots of microsphere position showing when feedback control system is off (left) and when feedback control system is on (right) which reduced the position variance of the microsphere by 60 %

Fourier analysis of the microsphere's position showed that the feedback control system acted to reduce disturbances that occurred within a time scale of 10 ms. This was limited by the hydro-dynamic response time of the microsphere to movement in the laser tweezers position, and could be improved by using smaller microspheres with a shorter response time.

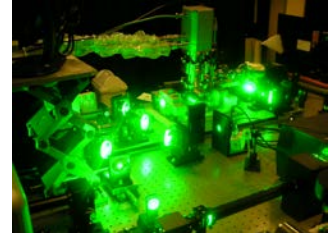
Acknowledgements

This work was funded by STFC Technology Transfer Partnership 2005-8. Active pixel sensor provided by MI3 Basic Technology programme.

References

1. M. Towrie et al, Rev. Sci. Instr. **80** 103704 (2009)

Molecular Structure & Dynamics in the Research Complex at Harwell



Contact Mike.Towrie@stfc.ac.uk

Mike Towrie

Central Laser Facility
Research Complex & Harwell

Gregory M. Greetham

Central Laser Facility
Research Complex & Harwell

Mark Pollard

Central Laser Facility
Research Complex & Harwell

Anthony.W. Parker

Central Laser Facility
Research Complex & Harwell

Ian P. Clark

Central Laser Facility
Research Complex & Harwell

Pierre Burgos

Central Laser Facility
Research Complex & Harwell

Vivan Sachdeva

Central Laser Facility
Research Complex & Harwell

Introduction

The move of the Molecular Structure and Dynamics, MSD, Group to the Research Complex at Harwell was completed successfully in November 2010. The ULTRA laser facilities are now housed in purpose designed laser and experimental stations with access to the shared facilities within the RCaH. This has increased facility capability in supporting high quality science, new facility developments, cross-campus research and collaborative experiments with resident RCaH research groups.

MSD Facilities

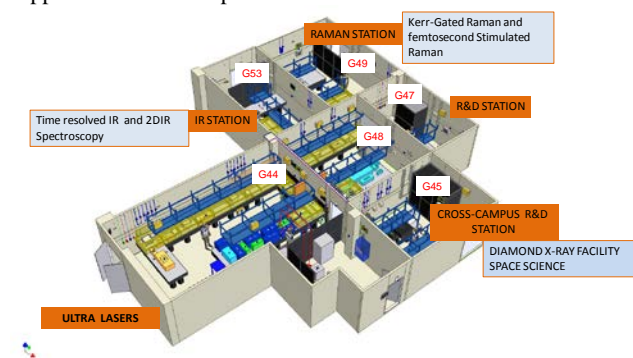
Figure 1 shows the new layout of the MSD facilities. A cluster of lasers lie at the heart. These are housed in two laser areas, G44 and G48. Light from any of the lasers in the cluster can be directed into four experimental stations. These are in turn,

IR Station (G53) - with time resolved infrared and ultrafast two dimensional IR spectroscopy facilities.

Raman Station (G49) - with time resolved Resonance Raman and femtosecond stimulated Raman spectroscopy facilities.

R&D station (G47) – with capacity to develop microscopy and spectroscopy facilities.

Cross-Campus R&D Station (G45) - housing Optical Tweezers, Raman microscope and ultrafast capabilities for support of Cross-Campus Activities.



The scientific operations are also supported by two workstations, G52 and G46 that interconnect to the experimental stations, biochemical and chemical preparation laboratories (G40 and G41) and the Diagnostic Laboratory with Fourier Transform Infrared (FTIR), UV to near infrared and fluorescence spectrometers.

The lasers

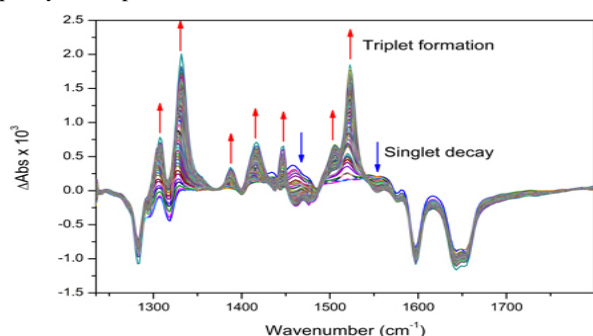
The cluster of lasers provides tremendous flexibility in approach allowing the spectroscopic techniques to be tailored to the experimental problems by using multiple beam configurations. The 10 kHz ULTRA system in G44 is at the core. This is a dual synchronized 10 kHz laser system¹ with 4 (or more) simultaneous picosecond and femtosecond optical parametric amplifier outputs tunable from the UV to mid IR. G44 also houses 10 kHz (& 10 Hz) nanosecond lasers that synchronise to the 10 kHz laser providing access to the nanosecond to microsecond time domain. This capability allows us to track molecular reactions from femtosecond timescales right through to microsecond timescales using ULTRA's very sensitive spectroscopic techniques and, importantly, under the same instrumental conditions². In G48, but sitting on the same optical bench as the 10 kHz lasers, is a 1 kHz high energy picosecond laser with 2 independent optical parametric amplifiers with UV to IR tunability. This, in the coming months, will synchronise to the 10 kHz laser to provide a 1 kHz laser pump pulse to initiate a reaction and to then probe the progress of the reaction using the 10 kHz light in a pump-probe-probe-probe.... configuration we call time resolved multiple probe spectroscopy (TR^MPS). In this way we can probe reactions using ultrafast non-linear spectroscopy techniques from picosecond to millisecond timescales.

The Infrared Station

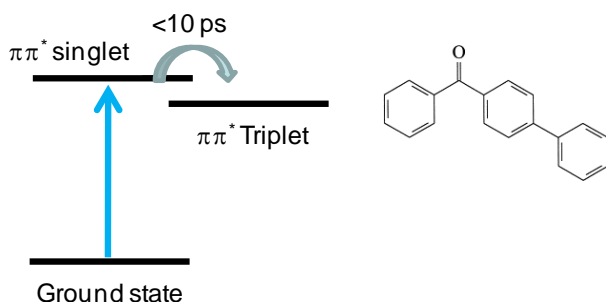
The IR station provides the state of the art in time resolved infrared spectroscopy and 2 options for ultrafast two dimensional IR spectroscopy. The spectrometer covers over 3 times greater spectral width and has 10 times faster acquisition than previous instruments of this type. Therefore, spectra that would have taken days to acquire now take minutes. This has opened up the techniques for the study of samples that have very weak signals. For example, as is typical for bio-molecular studies and on the studies of short lived intermediate states of molecular species that are present in low yield in the sample. Examples of the work carried out in this laboratory can be found in references and articles within this Annual Report.

Time Resolved IR spectroscopy (TRIR) - The nuclei in molecules are linked by bonds and every molecule has characteristic vibrations that are related to the strength of these bonds and the masses of the nuclei involved. The vibrations have energies that match the infrared region of the

electromagnetic spectrum and therefore IR light can probe them by measuring changes in the infrared light as it interacts with the molecules and from this one obtains information on the structure and dynamics of molecules as they react. The basic principle of TRIR (and 2DIR) is to measure changes in the intensity of a pulsed femtosecond IR beam as it passes through a sample after it has been excited (pumped) by one (or more) ultrashort light pulses timed with respect to the probe to accuracies of a few femtoseconds. The excitation may be with high energy photons (UV to near IR) to send molecules into excited electronic states or with low energy photons (IR) to excite vibrational states. The time evolution of the reaction is tracked by changing the relative timing between the pump beam (or beams) and the IR probe beam to generate a set of spectra at different time delays, this is called pump-probe spectroscopy. The IR spectra generated in this way contain a rich source of information on not only structure, but on the electronic state of a molecule and on how it is interacting with its environment, i.e. neighbouring molecules in condensed phase. Currently the TRIR and 2DIR instruments are able to cover a spectral energy range from 1200 cm^{-1} to 4000 cm^{-1} wavenumbers (8333 nm to 2500 nm) in spectral windows of 500 cm^{-1} . The range between 1200 cm^{-1} to 1700 cm^{-1} wavenumbers is within the so called fingerprint region of the IR spectrum and for most organic molecular species carries the most spectral information. As an example of the technique Fig. 3 shows the TRIR spectra of phenylbenzophenone dissolved in ethanol.



Phenylbenzophenone molecules in the solution are excited by 266 nm light into an excited state (singlet $\pi\pi^*$) which then relaxes to a new state (triplet $\pi\pi^*$) within 10 ps . The spectra are displayed as difference spectra, i.e. the difference in transmission of the probe when the sample is not pumped and when it is pumped. In addition to the positive signals created by the appearance of the triplet and singlet states there also appears



negative signals due to the removal of molecules from the initial ground state. Therefore, in this set of TRIR spectra we can track the population dynamics of 3 molecular states at once, the ground, singlet and triplet. It can be seen that there are large changes in the positions of the vibrational modes on excitation. For example the ground state mode at 1650 cm^{-1} due to the carbon to oxygen (C=O) vibrational mode appears to have shifted down to 1520 cm^{-1} in the triplet state. This has also been observed using time resolved Raman spectroscopy by other groups.

In order to improve signal to noise we pump the sample at 5000 kHz (on alternate probe laser pulses) and in this way we sample well above the frequency of unwanted noise signals from

laboratory sources, such as 50 and 100 Hz electrical supply noise and optical table vibrations.

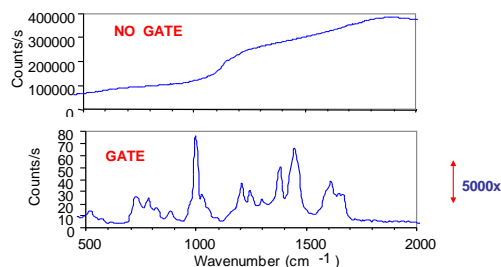
Ultrafast 2DIR - As the name suggests ultrafast 2DIR spectroscopy adds another dimension to IR spectroscopy. Conventional TRIR and IR spectroscopy has its limitations. For example we observe static features and changes in the shapes of vibrational spectral lines that cannot be interpreted with conventional infrared spectroscopy. These features may be due to processes such as inhomogeneous broadening that occurs when molecules find themselves in different local environments, molecular cooling processes or the influence that one vibrational mode within the molecule has on another, in other words vibrational mode coupling. These processes are extremely important in defining the dynamic (reactive) properties of molecules. For example vibrational mode coupling is the process that allows energy to flow within and between molecules. Ultrafast 2DIR spectroscopy provides a means to probe mode coupling directly and to observe vibrational energy exchange within the molecule and from the molecule to neighbouring molecules. Currently we use two (of many possible) 2DIR techniques. The first uses a picosecond IR light tuned to excite specific vibrational resonances within the molecules under study. Then with the broadband femtosecond probe pulse we probe many modes within the molecule to observe how the picosecond excitation of specific modes effect others as a function of time delay between the IR pump and probe. Other modes that are coupled or receive energy from the excited mode will be observed through changes in the transmission of the probe beam at the positions of the vibrational modes frequencies, so called off-diagonal signals. The wavelength of the IR excitation beam is then scanned to generate a 2D picture of how all the modes interact with each other. By collecting 2DIR spectra at a range of time delays a kinetic picture of the vibrational relaxations and couplings can be produced. In this way we have been able to monitor the mode coupling and vibrational relaxation of transient molecular species created on the ULTRA system.³ The second technique currently being commissioned is IR photon echo that measures interferences between the probe and coherent signals induced in the sample by two interfering pump beams. This technique uses three IR pulses of $<100\text{ fs}$ femtosecond pulse duration. This, while technically more challenging than the picosecond pump method has the advantage that it has faster time resolution and is therefore able to track faster energy exchange processes such as those known to occur in biomolecular systems. A report on this work can be found in this annual report.

The Raman Station.

The time resolved Resonance Raman and femtosecond stimulated Raman spectroscopy facilities are currently being re-commissioned within the RCaH and the first scheduled experiments using fs-stimulated Raman spectroscopy have begun. Time resolved Raman spectroscopy is the complementary technique to infrared spectroscopy. Its main advantages over time resolved infrared spectroscopy is 1) that it can probe specific electronic states of molecules using enhancements in signals that occur when the Raman excitation laser wavelength is tuned on to (i.e. resonant) with an electronic state of the molecule. This provides a means to choose which reactive molecular species to probe during a reaction by tuning the Raman excitation wavelength. 2) that it can cover a very broad vibrational energy range from 200 cm^{-1} (low frequency molecular vibrations such as bends and twists) to 3000 cm^{-1} the stretch vibrations of strong molecular bonds a range not possible with current IR technology. 3) that it does not suffer from absorption of the probe light by the solvent which is often a great obstacle to TRIR spectroscopy.

However, a major obstacle to Raman spectroscopy is that the Raman signals are usually feeble (a few photons per second per vibrational mode). This when combined with the fact that

samples often fluoresce strongly (at the thousands of photons per second level) creates a serious limitation to the application of the technique. We have two techniques to counteract this problem. We developed the first which is the Kerr Gated Raman method.⁴ Here a 4 ps optical gate picks out the Raman signal and suppresses the fluorescence signal by up to 10,000 times. The figure below shows with and without Kerr gated Raman of a petroleum fuel showing almost complete suppression of the fluorescence signal that swamps the Raman signal underneath.



The second method is the fs-stimulated Raman technique that uses a coherent interaction between two beams (a narrow band picosecond pulse (~2 ps, 12 cm⁻¹ bandwidth) and a broadband femtosecond pulse (<100 fs, >6000 cm⁻¹) and the molecules under study. The Raman signal appears as a small loss or gain signal that sit on top of the broadband pulse spectrum at positions of the Raman active modes of the sample. In principle the signals are detected in the same way as those for TRIR but using UV to near IR sensitive detectors instead of IR detectors. By modulating the picosecond pulse (Raman pump pulse) at 5 kHz we can see very small spectral changes in the 10 kHz femtosecond probe pulse at the 1 part in 10³ level. Since the intensity of the femtosecond probe pulse is well above that of the ambient fluorescence signals it is possible to generate Raman spectra from even the most intensely fluorescent samples. The tunability of the picosecond system allows us to select which Raman pump wavelength to excite at to take advantage of resonance enhancement or to minimize background signals.

R&D station

The R&D station is available to support facility developments, new techniques, RCaH and cross-campus research and to test feasibility for future new scientific experiments. Any of the beams in G44 and G48 may be made available in this area, which also houses a microscope.

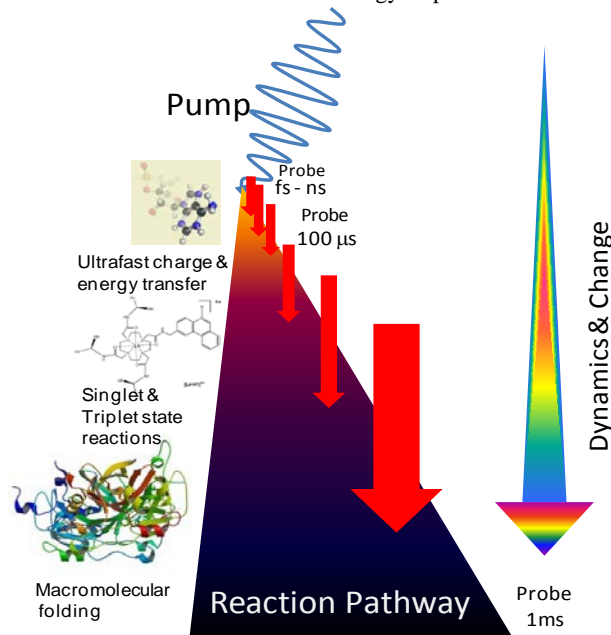
Cross-Campus R&D Station

There is an “optical bridge” between this laboratory and the G48 laser areas that will enable any one (or two) beams in G44 and G48 to be delivered to this area. It is envisaged that this will support cross-campus activities which would benefit from combined optical tweezers, microscope and ultrafast lasers. For example in probing fast chemical processes in water droplets or as optical manipulation tools, or to trigger crystal formation. More details on the science and developments in this station can be found in this annual report.

Time Resolved Multiple Probe Spectroscopy (TR^MPS)

The re-siting of the ultrafast laser facilities in the RCaH has enabled a new facility development TR^MPS funded through an STFC Facility Development grant. The aim of this project is to use the high energy 1 kHz laser in conjunction with the 10 kHz lasers to probe reactions from the earliest picosecond molecular dynamics and to track the progress of the reaction right out into the millisecond timescales. In this way we will see the earliest fast intramolecular dynamics of the molecules as they begin to react as well as the later evolution of the reaction involving, for example, large scale molecular structural changes, such as protein folding, or the diffusion of reactant species within

solution prior to undergoing further reactions. The complex timing control methods are currently being developed for this in collaboration with the STFC Technology Department.



Conclusions

The MSD has a cluster of lasers that create highly flexible light sources for the development and application of advanced vibrational spectroscopy techniques. This supports a wide range of interdisciplinary science programs within the UK and Europe and within the Research Complex at Harwell, underpinning its remit to encourage research projects utilizing the large scale facilities available on the Oxford and Harwell Campus.

Acknowledgements

We would like to acknowledge BBSRC and STFC for the funding for ULTRA and Mike George (Nottingham University) who was principle investigator on the ULTRA project. Simon Phillips and the RCaH support staff for their support during the move to the Research Complex at Harwell.

References

- ¹ *ULTRA: A Unique Instrument for Time-Resolved Spectroscopy*. GM Greetham, P Burgos, Q Cao, IP Clark, PS Codd, RC Farrow, et al. *Appl Spectrosc* **64** (12) 1311-1319 (2010)
- ² *A high-sensitivity femtosecond to microsecond time-resolved infrared vibrational spectrometer*. Towrie M, Gabrielson A, Matousek P, Parker AW, Rodriguez AM, Vlcek A Jr. *Appl Spectrosc*. **59**(4) 467 (2005).
- ³ *Investigating the vibrational dynamics of a 17e(-) metalcarbonyl intermediate using ultrafast two dimensional infrared spectroscopy* Kania, R; Stewart, AI; Clark, IP, et al. *PHYSICAL CHEMISTRY CHEMICAL PHYSICS* **12**(5) 1051-1063 (2010)
- ⁴ *Efficient Rejection of Fluorescence from Raman Spectra Using Picosecond Kerr Gating*. P. Matousek, M. Towrie, A. Stanley, and A. W. Parker. *Applied Spectroscopy*, **53**(12), 1485-1489 (1999)

Cross-Facility Research Activities in the Lasers for Science Facility

Contact andy.ward@stfc.ac.uk

Andy Ward

Lasers for Science Facility
Research Complex at Harwell

Introduction

The relocation of the Lasers for Science Facility (LSF) to the Research Complex at Harwell (RC@H) has seen an increase in the number of collaborations and projects that are running across multiple STFC facilities and Diamond Light Source. The science is largely of a multi-disciplinary nature and typically focuses on cross-cutting themes rather than specific facility techniques. As such, the topics are aligned with the scientific challenges addressed by the STFC Futures programme. A review of the current cross-Facility projects are briefly discussed here with reference made to the principal contacts should more detail be required.

The scope of activities falls into two general areas. The first consists of campus based scientists who have teamed up with the intention of extending the technical capability of their facilities and therefore allow new science to be performed. The second category involves academics who wish to utilize expertise and techniques of the LSF in combination with other facilities in a complementary approach to addressing their specific research needs.

Diamond I24: Optical loading of micro-crystals for X-ray diffraction studies.

Armin Wagner (DLS), Andy Ward (CLF), Bob Stevens (MNTC)

The collaboration includes the LSF, Diamond Light Source and STFC Micro and Nano Technology Centre, together with Zeiss Microimaging. The team have been granted beam time at the laser tweezers facilities in the LSF, Diamond beamline I24 and been funded by an STFC Innovations Proof-of-Concept grant to enable custom manufacture of novel micromesh designs.

The scientific challenge is to make X-ray diffraction studies on protein micro-crystals more accessible. Proteins can be difficult to crystallize and occasionally only micro-crystals are produced i.e. crystals with a size range between 1 and 10 microns. Crystals at the larger end of this distribution are still useful for obtaining X-ray diffraction data but are scarce and difficult to handle.

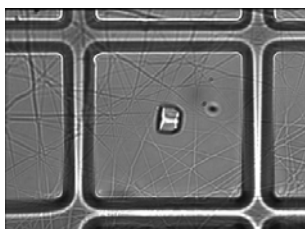


Figure 1. An optically loaded protein crystals (size approx. 10 microns) positioned onto fiber coated micromeshes of 50 micron aperture.

The research team used an optical trapping process for selecting specific protein crystals; capturing and then manipulating the crystal on to a custom micromesh (see Figure 1). The optical trap uses a tightly focused laser beam to create a balance between the scattering and refractive forces acting on the crystal. The overall force was sufficient to move the crystal at velocities in excess of 200 microns per second. To simplify the mounting process an electro-spun fiber was coated on the

micromesh which also enabled the crystals to remain in place during cryogenic freezing of the mesh in liquid nitrogen.

The first results were obtained from polyhedra crystals where the laser tweezers enabled the selection of crystals with dimensions larger than 8 microns. Reflections could be observed up to 1.2 Å (see Figure 2) and a complete data set up to 1.5 Å was obtained in an afternoon from in total 6 crystals. Initial indications are that even prolonged laser trapping with a 50 mW, 1064 nm beam has no discernable effect on the protein crystal.

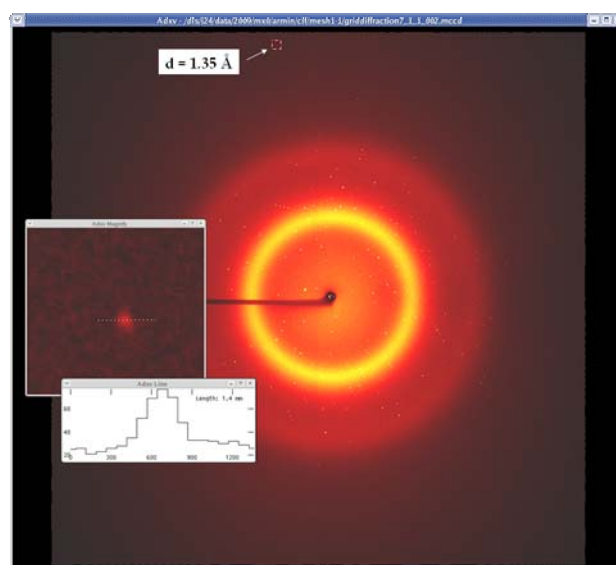


Figure 2. X-ray scattering data from an optically loaded crystal using the I24 beamline

The benefit from a facility perspective is that a process is now in place for mounting small crystals and obtaining datasets on I24 in hours rather than over months.

Diamond B23: Protein Folding

Robert Freedman (University of Warwick), Dave Clarke (CLF)

Producing a model for Protein disulphideisomerase (PDI) activity within cells requires a spectrum of advanced imaging techniques. PDI is the key element of the machinery which ensures correct and efficient folding of proteins exported by cells. These exported proteins include hormones, antibodies, growth factors and blood-clotting proteins and many of them are now being developed as protein pharmaceuticals.

The researchers are combining single molecule fluorescence resonance energy transfer (FRET) data from the LSF Octopus Cluster with the high sensitivity of synchrotron radiation circular dichroism on beamline B23. The collaboration has enabled measurement of intra-molecular distance distributions within the protein folding catalyst in comparison to the dynamics of conformational changes occurring during enzyme-substrate interactions. The clear benefit from multi-facility access is that complementary structural and dynamic

information on the same system can be used to build a detailed picture of PDI activity.

Diamond I22: A dual-beam laser trap for detailed X-ray studies in biology

Nick Terrill (DLS), Jen Hiller (DLS), Andy Ward (CLF)

An STFC Facility Development grant (ST/F001746/1) has funded the Central Laser Facility and Diamond Light Source to collaborate on the construction of a long working-distance dual-beam counter-propagating optical trap for the I22 microfoc end station. By extending the optical trapping field to several millimetres from the nearest lens the research team has opened the possibility for using optical manipulation as a complex sample handling and alignment tool for X-ray scattering studies.

The concept is to use two aligned microscope objective lenses to focus counter-propagating laser beams and generate an optical trapping field, which operates through opposed scattering forces, at a working distance of 17 mm. The equipment has been integrated into the microfoc end station on beamline I22 at Diamond Light Source which uses a focused X-ray beam approximately 10 microns in size to generate small angle X-ray scattering (SAXS). The optical trap holds and aligns objects such as single cells and macromolecules, into the X-ray beam. Figure 3 illustrates the results from the first test run in where data was obtained from an optically trapped zeolite sample.

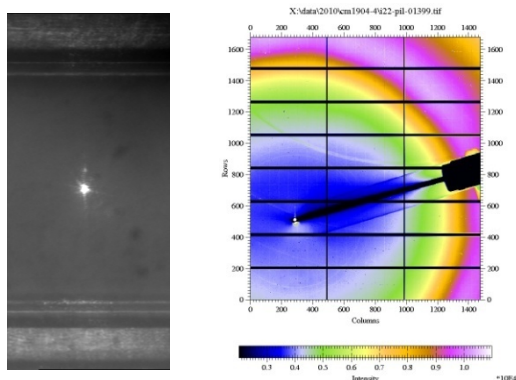


Figure 3. (Left) Image of trapped 9 micron bead from the perspective of the in-line microscope on the I22 beam line. A filter has been removed to allow the object to scatter laser light into the camera. (Right). An X-ray scattering pattern from the zeolite particle.

Diamond B16 and I15: Determination of the biological Bragg peak

Fred Currell (Queens University Belfast), Stan Botchway (CLF),

Advanced imaging techniques are central to this cross-Facility programme using a combination of confocal, multiphoton and FLIM microscopy, X-ray irradiation of samples on Diamond Beamlines B16 and I15, and cell culture work in the RC@H.

The concept is based on the ability of high atomic number (Z) materials, such as gold, to preferentially absorb kilovoltage X-rays compared to soft tissue. By controlling uptake of gold nanoparticles in cells it may be possible to achieve local dose enhancement in tumours during treatment with ionizing radiation. There is a need for extensive characterization of the responses to gold nanoparticles when assessing dose enhancing potential in cancer therapy. These complementary studies are increasing the understanding of how to enhance radiation effectiveness for radiotherapy with nano-Gold and also giving the first measurements related to the biological Bragg peak in living matter, something of central importance to radiation physics and biology.

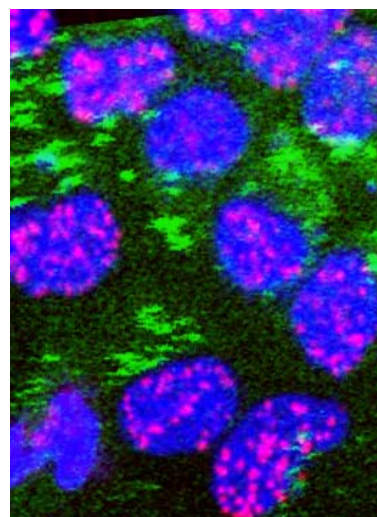


Figure 4. Confocal microscope image showing MDA-MB-231 breast cancer cells irradiated at Diamond Beam line B16, after doping with gold nanoparticles. The green shows the gold, imaged using multiphoton FLIM. The blue shows the nuclei and the magenta shows DNA damage resulting from radiation, taking using immunofluorescence confocal microscopy.

Diamond B24: Selective damage in protein crystals

Frank von Delft (Oxford), Robin Owen (DLS), Danny Axford (DLS), Mike Towrie (CLF), Andy Ward (CLF)

Damaging protein crystals, using an ultraviolet laser beam, may enable *in-situ* structural changes (phasing) in a crystal to be revealed through differences in X-ray diffraction. Phasing is significant because it can be used to complement diffraction intensities and build more complete structural datasets.

A short study was performed using a 266 nm laser installed into the experimental hutch of beamline I24. The researchers were interested in selective damaging of C-S bonds in protein crystals using UV irradiation of crystals of 8 different proteins. In certain crystals sulphur atoms did indeed disappear observably fast, but equally significant, was the observation that UV light also induced general decay of diffraction very similar to that induced by X-rays, (Figure 5).

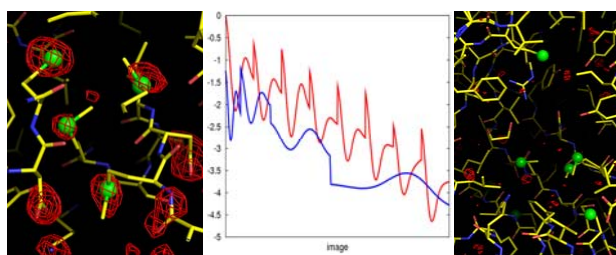


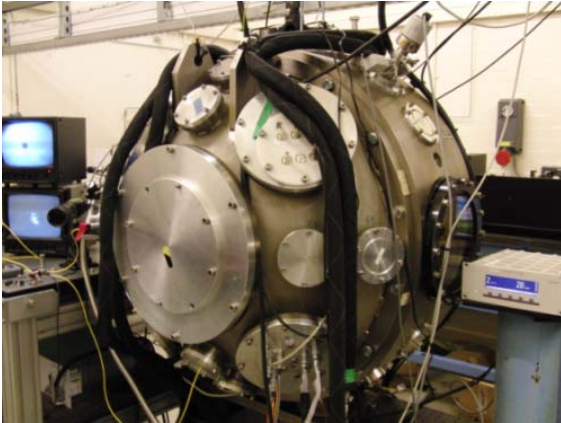
Figure 5: Damage effects of 266 nm laser light on crystals and diffraction. (a) Difference electron density showing disappearance (red mesh) of sulphur (green sphere) and other atoms in a crystal of CECR2 after 33min of UV exposure. (b) Significant overall loss of diffraction in a crystal of LCN15 induced by X-rays (red) and 266nm laser (blue). X-axis is dose in nominal units (10min UV). (c) Difference density of LCN15 after 42min UV, showing no specific damage, due to noise of general damage.

These initial studies provided interesting results and sufficient data to support an application for more beamtime at the LSF

CLF High Power: LIBRA target levitation

Dave Neely (CLF), Martin Tolley (CLF), Andy Ward (CLF)

An EPSRC Basic Technology grant entitled Laser Induced Beams of Radiation and their Application (LIBRA) has enabled collaboration between High Power Lasers and the LSF in the area of target manipulation. The targetry work package of LIBRA aims to levitate micron-scale targets, under vacuum, using photonic forces from lasers. Targets can then be manipulated with micron accuracy into the beam path of a high power laser for ion-beam production. In practice, this requires the construction of an optical trap inside a vacuum chamber (see Figure 6)



LIBRA

EPSRC
Pioneering research
and skills

Figure 6: The vacuum chamber and diagnostics. Monitors on the far left show a trapped droplet (top) and the laser focal profile (bottom)

To date we have successfully delivered and held a microscopic liquid droplet in the centre of a vacuum interaction chamber at 5 mbar using focused 1064 nm laser light to levitate the droplet. Droplets can be held to a precision of 1 micron making the laser levitation method suitable for co-alignment with a second “drive” laser.

Conclusions

There are a range of projects within the LSF that now have a common theme of using multiple facilities across the Harwell Campus. Further programmes, based on the award of NERC funded PhD studentships to use ISIS and Diamond, are being planned. In addition, the Research Complex at Harwell accommodates EPSRC funded residents who are keen to use STFC facilities. The LSF is active in encouraging the development of laser based techniques to enhance facilities and deliver new science and are receptive to any new lines of enquiry.